Hindawi
Advances in Civil Engineering
Volume 2022, Article ID 9259093, 11 pages
https://doi.org/10.1155/2022/9259093

Research Article

Numerical and Larg-Scale Laboratory Study of Rock Column Groups in Sandy Soil Behavior Improvement

Ali Yousefi Samangani and Reza Naderi

Civil Engineering Department, Shahrood University of Technology, Shahrood, Iran

Correspondence should be addressed to Ali Yousefi Samangani; aliyosefi90@yahoo.com

Received 24 May 2022; Revised 9 June 2022; Accepted 21 June 2022; Published 1 August 2022

Academic Editor: S. Mahdi S. Kolbadi

The use of stone columns as one of the effective methods in improving soil behavior can increase soil bearing capacity. One of the common methods in improving poor soil is the use of stone columns. Stone columns are considered one of the suitable options to improve the bearing capacity of loose cohesive and granular soils, which, in addition to reducing soil subsidence, is also considered an effective, economical, and environmentally friendly method in structures built on soil. Considering the financial and human losses caused by the construction of various buildings on poor soils, the importance of developing improvement methods in weak and unsuitable soils is essential. On the other hand, sandy soils are always considered an unsuitable soil sample in design. Therefore, in the present study, we use group stone columns to improve the behavior of a sandy soil sample. When a sample of soft sandy soil is exposed to loading due to its sandiness, we see an increase in soil subsidence and thus a decrease in its load-bearing capacity. In order to obtain practical and useable results in practice, in addition to numerical studies, we conduct a laboratory study to investigate the effect of rock columns on improving sandy soil performance. In sandy soil armed with 4 rock columns, the comparison of the results obtained from the numerical and laboratory model to the displacement of 2 mm is completely consistent with each other, and with increasing displacement, we see a difference between the numerical and laboratory results, so that for a 6 mm displacement, we see an 8% difference in numerical and laboratory results. The final sample capacity in the numerical and laboratory study in this case is 6730 N and 6192 N, respectively.

1. Introduction

To arrange the stone columns (single arrangement, triangular arrangement, and quadrangular arrangement), geometric characteristics of the stone columns (height, diameter of the column, center-to-center distance of the columns, and percentage of sandy soil density) are considered the main variables in the study. It should be noted that, in order to apply the results of the present study, in addition to performing a numerical study in finite element software, the samples will also be studied in a laboratory. In the process of designing the foundation of structures on different soils, bearing capacity and soil subsidence are considered the two main criteria considered by engineers and designers so that the construction of structures on soft and weak soils causes destructive subsidence and the instability of the structure. Therefore, it is necessary to develop methods for improving weak and unsuitable soils. On the other hand, sandy soils, especially in coastal areas, due to the poor mechanical properties of the soil, have always been considered an unsuitable soil sample in the design, and the need for improvement in this type of soil is urgently needed. Therefore, the present study, by using group stone columns, will seek to improve the behavior of a sample of sandy soil (Firoozkooh sandy soil). In fact, the present study will seek to improve sandy soil using group stone columns. Soil improvement is a process in which an increase in soil quality is observed. In other words, in the process of soil improvement, the mechanical and resistance parameters of the soil increase. In order to improve the behavior of sandy soils, the present study will deal with numerical and laboratory modeling of the group of rock columns as one of the appropriate tools for improving poor soils.

Among the various methods of deep vibration, we can name the method of stone or sand columns and the method of adding various dominant elements. In different conditions, according to the characteristics of the land for the construction of the structure and also according to the time and economic factors, the optimal method for improving poor soil can be selected. Currently, the stone column method is applied in a wide range of soil types, especially weak soils. As a simple and complete definition of a rock column, it can be said that the replacement of a part of weak soil by compacted vertical columns consisting of granular materials in a regular and completely permeable set in soil layers is called rock or sand columns. Figure 1 shows the geometric characteristics of group stone columns along with a sample of a single rock column in the soil bed. In this figure, H is the height of the rock column, L is the height of the loose soil layer, S is the center-to-center distance of the rock columns, and D is the diameter of the rock column. Determining the mentioned parameters in each issue optimally can have a significant effect on increasing soil efficiency and reduce destructive settlements in the soil. In these conditions, by reducing the possible damage due to soil weakness, the stability of the structure will be provided. Figure 1 shows the arrangement and number of individual stone columns used to form the group of stone columns. Therefore, it can be seen that group stone columns can have triangular arrangement (triple), square (quadruple), and rhombus (quadruple and not triple).

Figure 1: Sample of a stone column made in laboratory conditions [1].

2. Literature and Research Background

The vibrating rock column method is an extension of the floating vibration method, which was introduced in Europe in 1930 as an economical method for compacting granular soils. In the vibration compaction method, loose granular soils, due to applied vibrations, lose their previous arrangement and settle in their densest state. The vibrating rod then vibrates into the soil with a jet of pressurized water. The soil particles in the vicinity of the vibrating rod are separated from each other, and the effective stress between them is zero. These particles are in the densest possible position due to the movements of the vibrating rod and their weight. Given that the grains are placed next to each other without applying special stress, the obtained density will be stable (Figure 2). It should be noted that, depending on the height of the rock column and based on the depth of the rock bed, the column can be supported with the end located in the rock bed or floating with the free end of the column in the ground, according to or Figure 2 to be implemented [3].

Shear failure due to the occurrence of cuts in rock columns and surrounding soils is considered one of the most important factors in the failure of lands reinforced with rock column group. Determining appropriate methods to increase resistance and prevent this failure requires accurate knowledge of the behavior of the reinforced soil and the parameters affecting it. Puncture of a stone column occurs when the length of the column is not long enough to transfer the load to the depth. Based on experimental observations, in short stone columns (length-to-diameter ratio less than 6), swelling occurs along the entire length of the column, and the column is punched in the clay. This pattern of deformation occurs more frequently in adjacent columns (columns with a high replacement surface ratio). The tall columns are significantly deformed in the upper part, while the lower part remains unchanged. This indicates that the lack of load transfer to the floor in tall columns will not cause puncture rupture and the occurrence of other rupture conditions such as swelling or cutting. Therefore, the length-to-diameter ratio of about 6 is considered the critical length of the rock column in the design [4]. The rupture will occur conically in the form of a general shear failure. Under these conditions, column deformation in various forms such as lateral expansion, punching, shear, and bending has been observed, but the failure of the rock column group is a general shear failure [5]. Failure due to buckling in the side columns of a group is possible when the column length is less than the critical length.

Extensive laboratory and numerical studies have been performed to calculate the critical length. The results of studies show that, in calculating the critical length of the column, the amplitude of strain in the column is dependent on the diameter of the foundation and is not related to the diameter of the column [6]. Yang et al. [7] examined the numerical model and the laboratory model of stone columns in nonplastic silt materials. The numerical model included the three-dimensional finite element model of the group of stone columns, and the laboratory model included centrifuge experiments with and without stone columns. The results of laboratory models confirmed the obtained numerical results, and both types of analyses showed a reduction in soil mass deformation when using stone columns. In 2014 [8], Castro studied a series of two-dimensional and three-dimensional finite element analyses to evaluate the performance of a group of stone columns under a rigid foundation. The results of this research showed that the number and arrangement of stone columns have the least effect on changes in the load-settling curve. He also showed that, in order to estimate the reduction of subsidence and the critical length of stone columns, the group of stone columns located under the foundation can be replaced with a stone column with an equivalent surface in the center of the

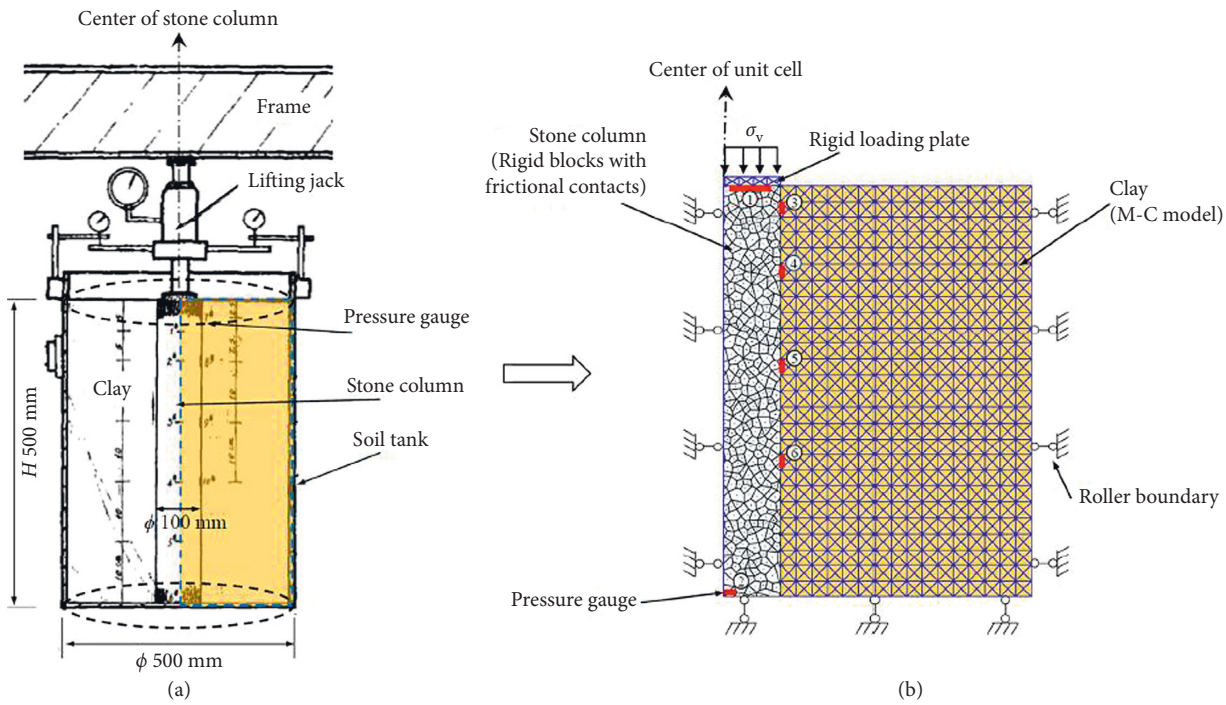

Figure 2: Conceptualization of the model from the experimental model to the numerical model. (a) Two-dimensional DEM-FDM model in UDEC [2]. (b) Experimental settings used.

foundation. In 2015, Mohapatara et al. [9] investigated the behavior of granular columns reinforced with geosynthetic fibers under a large-scale direct shear test. In the research of these researchers, sandy soil was used instead of ordinary solidified clay due to the simplicity of sample making. According to the results, it was observed that the presence of geosynthetic coating increases the bearing capacity of granular columns, but after rupture, the resistance to the surface of unreinforced granular columns decreases, and the mode of rupture of reinforced granular columns was of the flexural type, while the unreinforced column was broken in the form of shear, and also the effect of the grain column group was better than the single column with the same cross section.

Tan and Chen performed a two-dimensional numerical study on a rock column in a clay layer using a paired DEM-FDM model similar to the one proposed by Indratna et al. [10]. Tan and Chen used the Universal Distinctive Element Code (UDEC), a 2D-DEM program developed primarily to demonstrate the behavior of discontinuous materials (such as seamstones and aggregate columns) exposed to static or dynamic forces. In UDEC, distinct blocks behave as rigid or deformable elements, which also allows the simulation of continuous materials. Tan and Chen simulated columnar aggregates at UDEC as convex (polygonal) discrete blocks randomly generated based on Veronese veins, while Mohr-Coulomb can be considered as a proper constitutive law (Figure 2). The advantage of this method implemented in UDEC is that the complex interaction between the grain column and the surrounding soil can be simulated in a single model without the need for supervised nodes to pair the DEM-FDM model. The numerical results were in good agreement with the experimental data of the laboratory, which indicates the potential of this proposed modeling method for further numerical studies to continue to improve the understanding of the behavior of columnar systems. However, this modeling framework offers significant limitations in terms of total free space ratio and relative density modeling. Using the Veronese block system, stone columns are produced in a zero-porosity packing arrangement, which represents a much denser compaction condition than stone columns. In addition, it is common in DEM models for micromechanical contact parameters to differ from those obtained from laboratory experiments. Therefore, appropriate calibrations are needed to ensure that the contact parameters model the reproduction of the behavior of the granular material. Next, a simple strain model is simulated. Hence, a full-scale three-dimensional DEM model can improve the understanding of the complex behavior of stone columns [11].

2.1. Research Methods. The modeling performed in the present study will be done in the form of numerical modeling and large-scale (physical) laboratory modeling. In numerical modeling using Abacus finite element software, rock column groups with different arrangement, number, and diameter of rock columns in sandy soil will be studied under load [12]. Also, in order to perform physical modeling in the laboratory environment, the necessary equipment for physical modeling of stone columns will be made, and loading will be done by a hydraulic Jack. In fact, the samples will be made in the laboratory and loaded first [13]. In physical modeling in the laboratory, after the construction of the device, circular stone

columns with different diameters, in different geometric arrangements and for different percentages of soil density, will be loaded by a hydraulic Jack [14]. During the experiment, two measurement tools will be used [15]. One of these tools will be used to measure displacement and the other to record and measure the load on the soil sample. In numerical modeling using Abacus finite element software, stone columns with different geometry and geometric arrangement in sandy soil, under the application of an axial force, will be studied. Finally, the most appropriate arrangement and geometric parameters of the rock column, which leads to the most optimal response of the soil mass under load, are introduced, and the results obtained from laboratory study and numerical modeling will be compared (Figure 3).

Introducing the studied samples, as mentioned so far, geometric characteristics, the arrangement of stone columns, and soil compaction percentage are considered variable parameters in the present study. Therefore, the studied models will be formed based on these variables [16]. Therefore, in the following, we will introduce the variables of the present study in detail. The basic variables in this study include the physical and mechanical properties of the various components [17]. The diameter of stone columns (d) is considered one of the variables of the present study. Therefore, three diameters of 60, 90, and 120 mm will be used as the diameters of the stone column. The height-to-diameter ratio of the stone columns (L/d) studied in the present study will be considered equal to 3, 5, and 7, and then the most appropriate height-to-diameter ratio based on the results obtained will be selected. Depending on the size of the proposed diameters, the length of the stone columns will be based on Table 1.

According to the introduced variables, 162 different modeling modes ($2 \times 3 \times 3 \times 3 \times 3$ modes) will be studied and evaluated in the present research in a software and laboratory environment. Table 2 presents the selected cases evaluated in the present study along with the acronym.

2.2. Laboratory Study. In order to perform laboratory studies, it is necessary to manufacture samples and test equipment. Therefore, in the following, we will pay attention to the details of making the device and making stone columns in the laboratory environment, along with introducing other types of required equipment and tools. Due to the fact that, in the present study, laboratory modeling is considered on a large scale, it is necessary to make a test box to estimate the behavior of the substrate in certain dimensions. In order to perform experiments on group stone columns with the desired arrangement, it is necessary to make the necessary equipment for testing; for this purpose, equipment similar to the equipment is provided [18], including a large metal box [19]. The dimensions of the test box mold made in the present study are $90 \times 120 \times 120$ cm. It should be noted that, after the construction of the device with the desired dimensions and considering that according to studies the wedge created under the foundation is spread to a distance of about 2 to 2.5 times the width of the foundation from the center of the foundation to the surrounding area, border conditions will not affect the results of large-scale experiments. Figure 4 shows the foundation simulator designed for laboratory studies in the present study. The loading system includes loading frame, load handling system, loading plate, and data collection system. The data collection system consists of a computer, data entry system, displacement meter, and dynamometer [20].

The test procedure is similar to the procedure performed in reference [21], which is described in detail in the following. Three-ton Jack is installed in order to apply load and displacement sensors and dynamometer in order to record the amount of displacement and force applied to the loading plate. The loading process is based on displacement control, and its speed is selected as 1 mm/min. It should be noted that the conditions for stopping the application of load to the

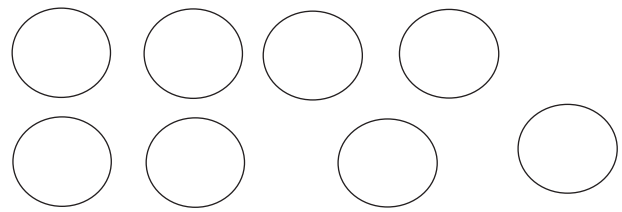

Figure 3: Geometric arrangement of stone columns studied in the present study.

Table 1: The length of the stone columns studied in the present study.

D (mm)	L/d = 3	L/d = 5	L/d = 7
60	180	300	420
90	270	450	630
120	360	600	840

Table 2: Introduction of the studied modes in the present study.

No.	Abb	D (cm)	H/D	Geo	Density (%)
1	$4SC_{6\text{-}5\text{-}0\text{-}2}$	6	5	4	0
2	$4SC_{6\text{-}5\text{-}0\text{-}3}$	6	5	4	0
3	$4S_{C6\text{-}5\text{-}35\text{-}2}$	6	5	4	35
4	$4SC_{6\text{-}7\text{-}0\text{-}2}$	6	7	4	0
5	$4SC_{6\text{-}7\text{-}0\text{-}3}$	6	7	4	0
6	$4SC_{12\text{-}5\text{-}0\text{-}2}$	12	5	4	0
7	$4SC_{12\text{-}5\text{-}0\text{-}3}$	12	5	4	0
8	$4SC_{12\text{-}5\text{-}35\text{-}2}$	12	5	4	35
9	$4SC_{12\text{-}7\text{-}0\text{-}2}$	12	7	4	0
10	$4SC_{12\text{-}7\text{-}0\text{-}3}$	2	7	4	0
11	$3SC_{6\text{-}5\text{-}0\text{-}2}$	6	5	3	0
12	$3SC_{6\text{-}5\text{-}0\text{-}3}$	6	5	3	0
13	$3SC_{6\text{-}5\text{-}35\text{-}2}$	6	5	3	35
14	$3SC_{6\text{-}7\text{-}0\text{-}2}$	6	7	3	0
15	$3SC_{6\text{-}7\text{-}0\text{-}3}$	6	7	3	0
16	$3SC_{12\text{-}5\text{-}0\text{-}2}$	12	5	3	0
17	$3SC_{12\text{-}5\text{-}0\text{-}3}$	2	5	3	0
18	$3SC_{12\text{-}5\text{-}35\text{-}2}$	12	5	3	35
19	$3SC_{12\text{-}7\text{-}0\text{-}2}$	2	7	3	0
20	$3SC_{12\text{-}7\text{-}0\text{-}3}$	12	7	3	0
21	$1SC_{6\text{-}5\text{-}0\text{-}0}$	6	5	1	0
22	$1SC_{6\text{-}5\text{-}35\text{-}0}$	6	5	1	35
23	$1SC_{6\text{-}7\text{-}0\text{-}0}$	6	7	1	0
24	$1SC_{12\text{-}5\text{-}0\text{-}0}$	12	5	1	0
25	$1SC_{12\text{-}5\text{-}35\text{-}0}$	12	5	1	35
26	$1SC_{12\text{-}7\text{-}0\text{-}0}$	12	7	1	0

Figure 4: Pi simulator for large-scale and load plate tests with displacement and dynamometer sensors.

samples, reaching the settling rate in the samples to the extent of 50 mm, are considered [22]. Also, the loading plate is positioned so that its center is on the center of the stone pillar. The ratio of height to diameter of the studied stone columns is considered to be equal to 3, 5, and 7, and then the most appropriate ratio of height to diameter will be selected based on the results obtained. In the present study, each experiment was repeated twice to ensure the accuracy of the experiments performed. It is important to note that, before making the samples, the inner walls of the test box (device) were well impregnated with oil to minimize the friction of sandy soil with the surfaces of the device under test [23].

Figure 4 shows how the displacement sensor and dynamometer are connected on the loading screen. In this study, in order to apply load on the studied stone columns, a circular steel loading plate has been used. A hydraulic Jack is applied to the center of the loading plate, and two displacement sensors record the amount of displacement recorded on the steel plate [24]. Also, by installing a dynamometer sensor at the point of contact of the Jack with the steel plate, the amount of force applied to the steel plate can be controlled and measured.

2.3. Material Specifications. The soil studied in the present study is Firoozkooh sandy soil. Therefore, stone columns enclosed in sandy soil will be studied and tested. The characteristics of the studied sandy soils are presented in Table 3.

2.4. Construction of Stone Columns. There are different methods for making stone columns. In this study, to make stone columns, a plastic sheath (thin-walled pipe) with different diameters was used, and during the construction of the model, at each stage, according to the specific weight of the column, the required sand was poured, and compaction operations were performed. And graveling was done. Figure 5 shows the steps of making a stone column. Table 4 presents the characteristics of the sand used to build the stone columns.

3. Numerical Study

The Mohr–Coulomb rupture model is a complete elasto-plastic model of the simplest and most widely used models in geotechnical analysis. This is because of the small number of variables without the need for complex experiments. In the Mohr model, the Mohr–Coulomb rupture criterion is used as the yield surface, and the law of flow in the shear state is assumed to be independent. In using this model, it should be noted that some basic aspects of soil behavior, such as the dependence of stiffness on the path and the history of stress

Table 3: Introducing the characteristics of the studied sandy soil.

Parameter	Numerical value
Dry specific gravity	16 kN/m^2
Saturation specific gravity	18 kN/m^2
Dry internal friction angle	40 degrees
Internal friction angle of saturation	36 degrees
Adhesion	0
Modulus of elasticity	40 MPa
Specific density	2.65
Poisson ratio	0.3
Maximum porosity ratio	0.6
Minimum porosity ratio	0.3

Figure 5: Steps of making a stone column in the laboratory.

and strain in it, have been omitted [13]. In order to model sandy soil and improve it by using stone columns with the desired specifications, the capabilities of Abacus finite element software will be used. In order to apply the load, a single load is used. The magnitude of the applied load will be a maximum of 3 tons. In geotechnical engineering, Mohr–Coulomb theory is used to determine the shear strength of soil and rock at different levels of effective stress, and in structural engineering, this theory is used to determine the load and fracture angle of concrete and similar materials. In addition, the Coulomb friction hypothesis is used to obtain the

Table 4: Introducing the specifications of sand used to build stone columns.

Parameter	Numerical value
Dry specific gravity	16 kN/m^2
Saturation specific gravity	19 kN/m^2
Dry internal friction angle	41 degrees
Internal friction angle of saturation	37 degrees
Adhesion	0
Modulus of elasticity	100 MPa
Specific density	2.6
Poisson ratio	0.2
Maximum porosity ratio	0.75
Minimum porosity ratio	0.35

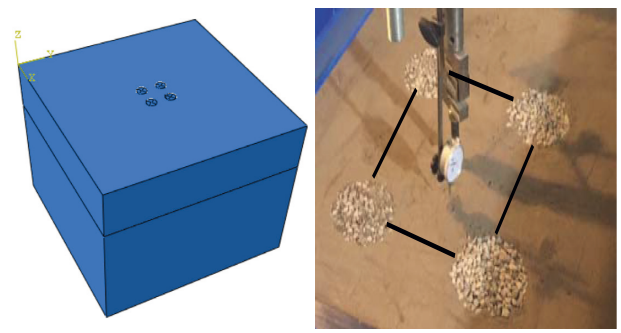

Figure 6: Sandy soil model reinforced with 4 stone pillars.

combination of normal and shear stresses that cause failure. The molar circle determines the main stresses that cause this combination and the angle of their action plane. If the failure of material occurs according to the Columbus friction hypothesis, the angle of the displacement line at the point of failure will be equal to the angle of friction. According to this property, the strength of the material can be calculated by comparing the external mechanical work resulting from external displacement and loading as well as the internal mechanical work resulting from stress and strain at the fracture line. According to the principle of energy conservation, the sum of these values must be zero. This makes it possible to calculate the structural failure load. One development of the Mohr–Coulomb model is the description of fractures isolated by combining Columbus's law of friction with Rankine's principle. The fracture criterion shows the linear coupling obtained from the shear strength diagram of the material against the normal stress applied to it. This criterion is defined as equation (1):

$$\tau = \sigma \tan(\varphi) + c. \tag{1}$$

3.1. Analysis of Results. In order to evaluate the performance of the group of rock columns in improving the behavior of sandy soil, in both experimental and numerical studies, different responses were recorded under a fixed and specific axial load and compared with each other in different modes. The analysis and interpretation of the results are made in such a way that the direct impact of each variable on the final response of the soil system dominated by the rock column is

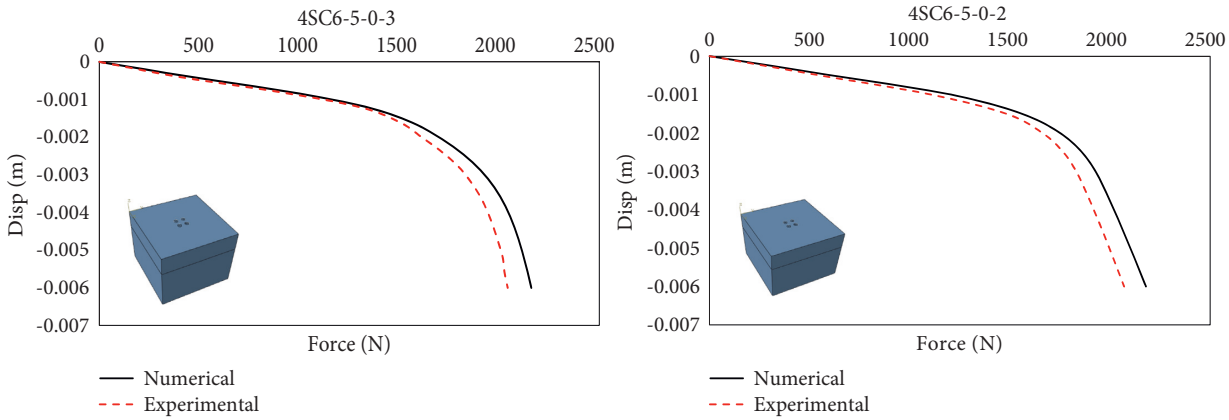

Figure 7: Conditional force-displacement diagram for 4SC6-5-0-2 and 4SC6-5-0-3 models in both numerical and laboratory modes.

understandable. The first answer studied in the present study is the comparison of force-displacement diagrams related to 26 selected models in both numerical and laboratory modes. According to the force-displacement diagram, the maximum bearing capacity and the maximum displacement created in the studied models can be compared with each other. It should be noted that, in naming the studied samples, the number before SC indicates the number of stone columns, and the numbers after SC indicate the diameter of the stone column, the ratio of height to diameter of the stone column, the percentage of soil density, and the distance from the center to the center of the column, respectively. The stones are from each other. Figure 6 shows the dominant soil with 4 stone columns in the software environment and in the laboratory environment. Also, in Figure 6, the force-displacement diagram of the sample 4SC6-5-0-2 is presented in both numerical and laboratory modes.

According to Figure 7, the results obtained from the numerical and laboratory study are in good agreement with each other, which indicates the acceptable accuracy of the modeling process in the software environment. Due to the fact that the load is applied statically and controlled by displacement, it is observed that, for a displacement of 6 mm, the final capacity of the sample is obtained based on a numerical study equal to 2179 Newtons, while the final capacity of the sample in 2070 Newton laboratory studies has been obtained. In this case, the difference between the results of numerical and laboratory studies on the 4SC6-5-0-2 model is equal to 5%. Figure 7 shows the force-displacement diagram of 4SC6-5-0-3 in both laboratory and numerical modes. Adaptation of numerical and laboratory results indicates the desired accuracy of the research process. In this case, the sandy soil is reinforced with 4 stone columns with a square arrangement. The diameter of the columns is 6 cm, the ratio of height to the diameter of the columns is equal to 5, and the distance from the center to the center of the stone columns is equal to 3. According to the results presented in Figure 7, for a displacement of 6 mm, the final sample capacity calculated from the numerical and laboratory analysis is 2159 and 2041 N, respectively. The difference between the results obtained from numerical and laboratory studies on the 4SC6-5-0-2 model is equal to 5.46%.

Figure 8 shows the force-displacement diagram for 4SC6-5-35-2 in both laboratory and numerical modes. In this case of modeling, we see the adaptation of numerical and laboratory results. The soil sample in this case consists of sandy soil with 4 stone columns with a square layout. In this sample, the diameter of the stone columns is 6 cm, and the height to diameter ratio of the columns is 5, the distance from the center to the center of the columns. The rock is considered to be equal to 2, and the soil density percentage is equal to 35%. Based on the results presented in Figure 8, it can be seen that the final sample capacity in the numerical and laboratory study for 6 mm displacement is estimated to be 2141 and 2012 newtons, respectively. The difference between the results obtained from numerical and laboratory studies on the 4SC6-5-35-2 model is equal to 6.02%. Figure 8 shows the force-displacement diagram of the 4SC6-7-0-2 sample in both laboratory and numerical modes. In this mode of modeling, there is an acceptable agreement between numerical and laboratory results. The soil sample in this case consists of sandy soil with 4 stone columns with a square layout. In this sample, the diameter of the stone columns is 6 cm, and the height to diameter ratio of the columns is 7, the distance from the center to the center of the columns. Stone is considered equal to 2, and soil without density is considered. Based on the results presented in Figure 8, it can be seen that the final capacity of the sample in the numerical and laboratory study for 6 mm displacement is estimated to be 2806 and 2609 N, respectively. The difference between the results of numerical and laboratory studies on this model is equal to 7%.

Figure 9 shows the force-displacement diagram of the 4SC6-7-0-3 sample in both laboratory and numerical modes. The soil sample studied in this case consists of sandy soil with 4 stone columns with a square arrangement. In this sample, the diameter of the stone columns is 6 cm, and the height to diameter ratio of the columns is 7, the distance from the center to the center of the columns. Rock is equal to 3, and soil without density is considered. The results show that the difference in bearing capacity in this case is based on two categories of numerical and laboratory studies equal to 7%. The final sample capacity in the numerical and laboratory study for a displacement of 6 mm is estimated at 2614 and 2431 N, respectively. Figure 9 shows the force-

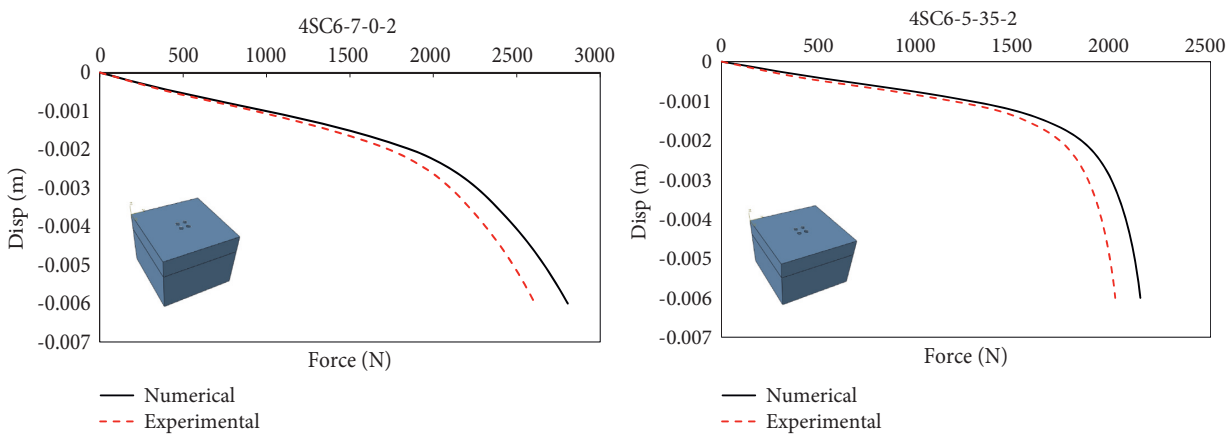

Figure 8: Force-displacement diagrams related to 4SC6-5-35-2 and 4SC6-7-0-2 models in both numerical and laboratory modes.

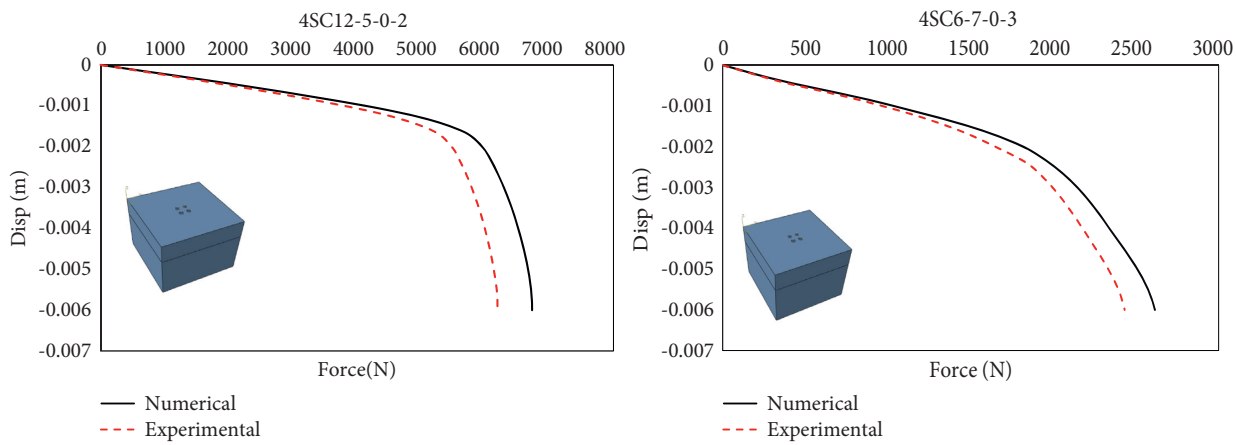

Figure 9: Force-displacement diagram related to models 4SC6-7-0-3 and 4SC12-5-0-2 in both numerical and laboratory modes.

Table 5: Numerical comparison of bearing capacity of numerical and laboratory models related to reinforced sandy soil samples.

Model	Numerical final load capacity (newton)	Final laboratory bearing capacity (newton)	Results difference (%)
$4SC_{6\text{-}5\text{-}0\text{-}2}$	2179	2070	5
$4SC_{6\text{-}5\text{-}0\text{-}3}$	2159	2041	5.46
$4SC_{6\text{-}5\text{-}35\text{-}2}$	2141	2012	6.02
$4SC_{6\text{-}7\text{-}0\text{-}2}$	2806	2609	7
$4SC_{6\text{-}7\text{-}0\text{-}3}$	2614	2431	7
$4SC_{12\text{-}5\text{-}0\text{-}2}$	6730	6192	8
$4SC_{12\text{-}5\text{-}0\text{-}3}$	6860	6517	5
$4SC_{12\text{-}5\text{-}35\text{-}2}$	6946	6543	5.8
$4SC_{12\text{-}7\text{-}0\text{-}2}$	6746	6206	8
$4SC_{12\text{-}7\text{-}0\text{-}3}$	9043	8410	6.9

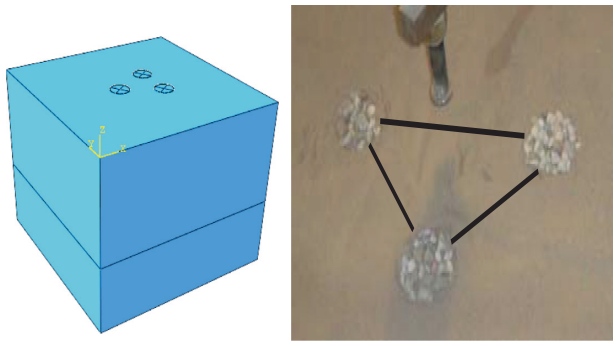

Figure 10: Sandy soil model reinforced with 3 stone pillars.

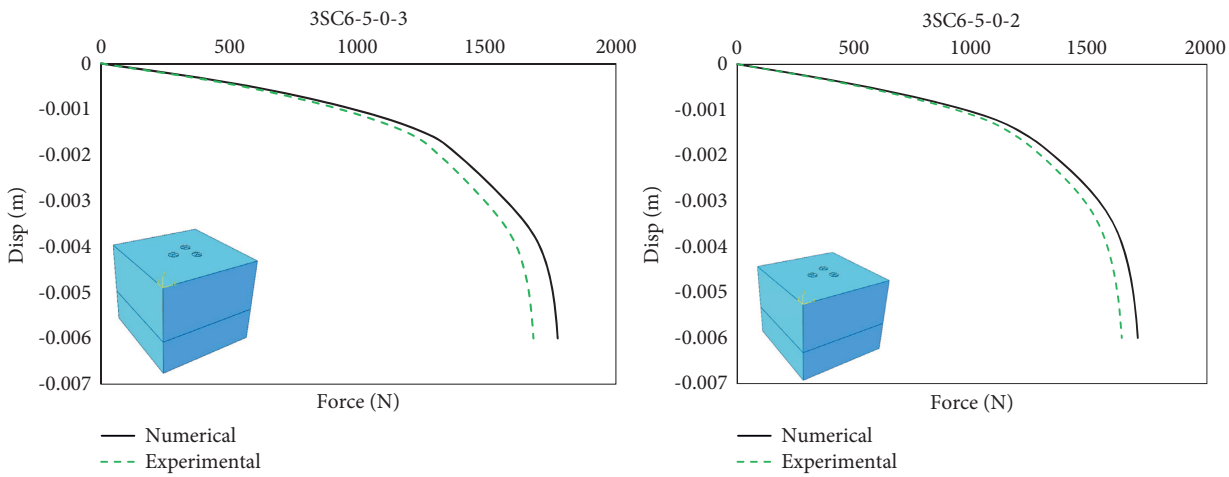

Figure 11: Force-displacement diagram related to 3SC6-5-0-2 and 3SC6-5-0-3 models in both numerical and laboratory modes.

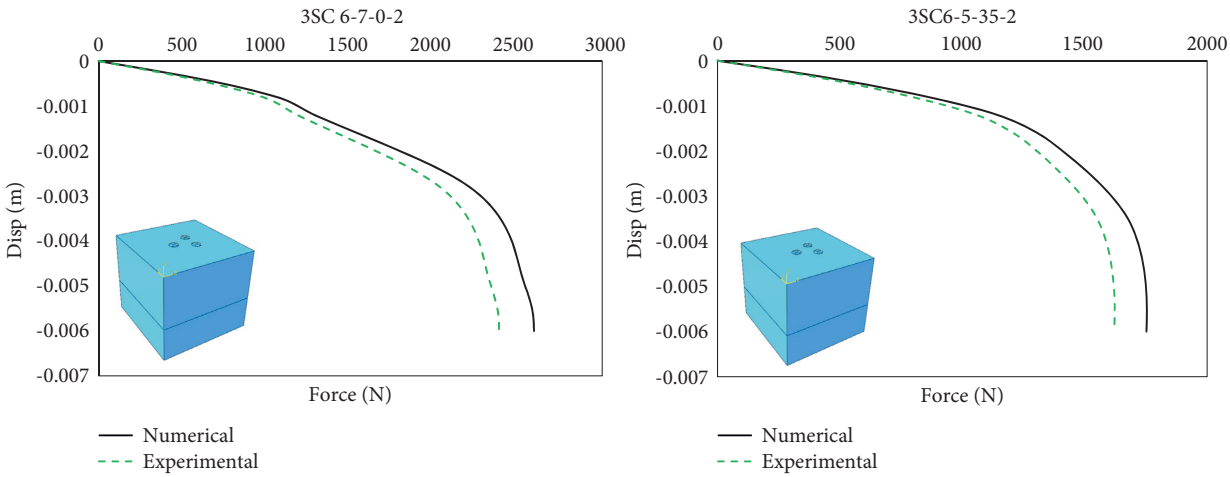

Figure 12: Force-displacement diagram related to models 3SC6-5-35-2 and 3SC6-7-0- in both numerical and laboratory modes.

displacement diagram of the 4SC12-5-0-2 sample in both laboratory and numerical modes. From the comparison of the results obtained from the numerical and laboratory model to the displacement of 2 mm completely on each other and consistent with increasing displacement, we see a difference between numerical and laboratory results so that, for a displacement of 6 mm, we will see an 8% difference in numerical and laboratory results. The final sample capacity in the numerical and laboratory study in this case is 6730 and 6192 N, respectively (Table 5).

Figure 10 shows the dominant soil with 3 stone columns in the software environment and in the laboratory environment. Also, in Figure 10, the force-displacement diagram related to sample 3 SC6-5-0-2 is presented in both numerical and laboratory modes.

Figure 11 shows the results of the numerical and laboratory study on sample 3 SC6-5-0-2. The obtained results indicate acceptable compatibility of laboratory and numerical results with each other, which indicates the acceptable accuracy of the modeling process in the software environment. It can be seen that, for a displacement of 6 mm, the final sample capacity is based on a numerical study of 1705 N, while the final sample capacity is obtained in laboratory studies at 1637 N. In this case, the difference between the results obtained from numerical and laboratory studies on the 3SC6-5-0-2 model is equal to 3.9%. Figure 11 shows the results of the numerical and laboratory study on sample 3 SC6-5-0-3. It can be seen that, for a displacement of 6 mm, the final sample capacity is based on a numerical study of 1773 newtons, while the final sample capacity is obtained in laboratory studies at 1679 newtons. In this case, the difference between the results of numerical and laboratory studies on the 3SC6-5-0-3 model is 5.3%.

Figure 12 shows the results of the numerical and laboratory study on sample 3 SC6-5-35-2. It can be seen that, for a displacement of 6 mm, the final sample capacity is based on a numerical study of 1752 N, while the final sample capacity in laboratory studies is 1620 N. In this case, the difference between the results of numerical and laboratory studies on the 3SC6-5-0-3 model is 7.53%. Figure 12 shows the results obtained from the numerical and laboratory study on sample 3 SC6-7-0-2. It can be seen that, for a displacement of 6 mm, the final sample capacity is based on a numerical study of 2594 newtons, while the final sample capacity is obtained in laboratory studies at 2386 newtons. In

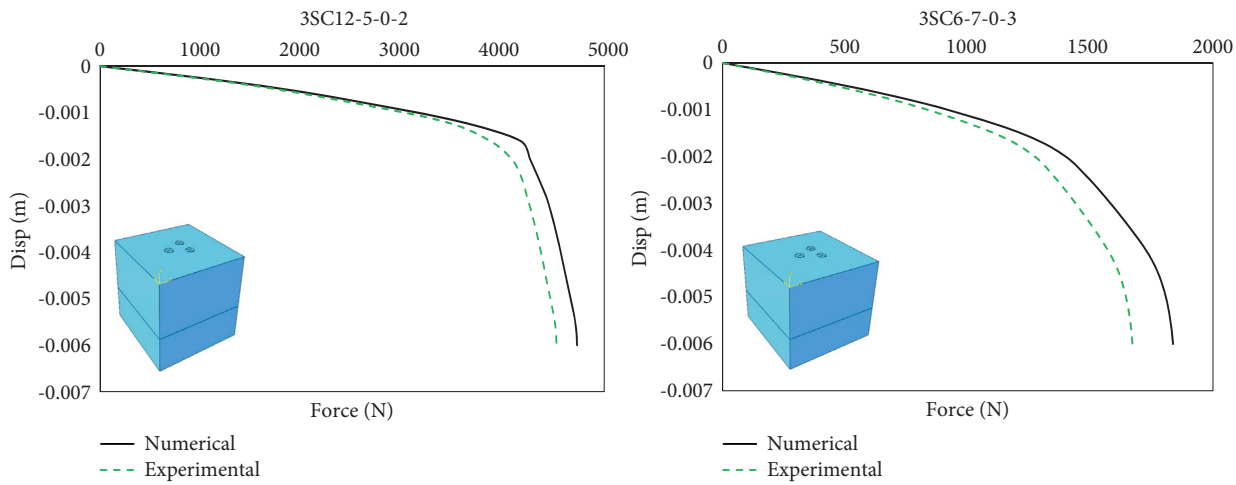

Figure 13: Force-displacement diagram related to model 3SC6-7-0-3 in both numerical and laboratory modes.

this case, the difference between the results obtained from numerical and laboratory studies on the 3SC6-7-0-2 model is equal to 8%.

Figure 13 shows the results of the numerical and laboratory study on sample 3 SC6-7-0-3. It can be seen that, for a displacement of 6 mm, the final sample capacity is based on a numerical study of 1837 newtons, while the final sample capacity is obtained in laboratory studies at 1671 newtons. In this case, the difference between the results obtained from numerical and laboratory studies on the 3SC6-7-0-2 model is equal to 9%. Figure 13 shows the results of the numerical and laboratory study on sample 3 SC12-5-0-2. It is observed that, for a displacement of 6 mm, the final sample capacity is obtained based on a numerical study equal to 4731 N, while the final sample capacity is obtained in laboratory studies at 4527 N. In this case, the difference between the results obtained from numerical and laboratory studies on the 3SC6-7-0-2 model is equal to 4.3%.

4. Discussion and Conclusion

The use of stone columns can be done individually or in groups. Due to the high volume of studies on the performance of individual rock columns, the present study sought to investigate the performance of group rock columns in improving the behavior of sandy soils. The soil sample studied in this study was sandy soil (Firoozkooh sandy soil), and also, in order to achieve real laboratory results, the experiments were performed as large-scale experiments. After this step, based on the results of experiments, numerical modeling will be performed using Abacus finite element software. Stone columns will be studied and evaluated in groups in different numbers and arrangements. The studied modes are in the form of a triangular triple group and a quadruple square group. The Mohr–Columb theory is a theory for describing the reaction of materials such as soil and concrete against normal shear stress. In most classical engineering materials, part of the shear failure cap somehow follows this theory. The scope of application of Mohr–Columb theory is for materials that have a much higher compressive strength than their tensile strength. The stone columns will be studied and evaluated as a group in different numbers and arrangements (triangular triple group, square quadruple group, and single arrangement). For the distance of stone columns in the group, the distance from the center to the center of the stone columns is 2, 2.5, and 3 times the diameter of the stone column. Sand soil density in the present study bed soil (Firoozkooh sand soil) was studied in two compaction states without density and with a density of 35%. In sandy soil reinforced with 3 stone pillars, it is observed that, for a displacement of 6 mm, the final sample capacity is obtained based on a numerical study equal to 4731 N, while the final sample capacity is obtained in laboratory studies of 4527 N.

Data Availability

Requests for access to these data should be made to the corresponding author's e-mail address: aliyosefi90@yahoo.com.

Conflicts of Interest

The authors declare that there are no conflicts of interest regarding the publication of this paper.

Authors' Contributions

Ali Yousefi Samangani contributed to FEM controlling, simulation controlling, results evaluation, and paper writing. Reza Naderi contributed to literature review, FEM simulation, and draft writing.

Acknowledgments

The authors would also like to show their gratitude to Dr. Amir Bazrafshan (Civil Engineering Dept., Shahrood University of Technology, Iran) for sharing his pearls of wisdom with them during the course of this research.

References

[1] M. Etezad, "Geotechnical performance of group of stone columns," PhD Thesis, Concordia University, Montreal, Canada, 2007.

[2] S. M. Seyed Kolbadi, N. Hassani, S. M. Seyed-Kolbadi, and M. Mirtaheri, "Analyzing parametric sensitivity on the cyclic behavior of steel shear walls," *Shock and Vibration*, vol. 2021, Article ID 3976793, 10 pages, 2021.

[3] A. Zahmatkesh and A. J. Choobbasti, "Investigation of bearing capacity and settlement of strip footing on clay reinforced with stone columns," *Australian Journal of Basic and Applied Sciences*, vol. 4, no. 8, pp. 3658–3668, 2010.

[4] B. Pulko and B. Majes, "Analytical method for the analysis of stone-columns according to the Rowe Dilatancy theory," *Acta Geotechnica Slovenica*, vol. 3, no. 1, pp. 37–45, 2006.

[5] M. Krishna and M. R. Madhav, "Engineering of ground for liquefaction mitigation using granular columnar inclusions: recent developments," *American Journal of Engineering and Applied Sciences*, vol. 2, no. 3, pp. 526–536, 2009.

[6] A. P. Ambily and S. R. Gandhi, "Behavior of stone columns based on experimental and FEM analysis," *Geotechnical and Geoenvironmental Engineering*, vol. 133, 2007.

[7] J. Castro, "Numerical modelling of stone columns beneath a rigid footing," *Computers and Geotechnics*, vol. 60, pp. 77–87, 2014.

[8] S. R. Mohapatra, K. Rajagopal, and J. Sharma, "Direct shear tests on geosynthetic-encased granular columns," *Geotextiles and Geomembranes*, vol. 44, no. 3, pp. 396–405, 2016.

[9] X. Tan, M. Zhao, and W. Chen, "Numerical simulation of a single stone column in soft clay using the discrete-element method," *International Journal of Geomechanics*, 2018.

[10] M. Kolbadi, "Review on nonlinear behavior assessment of reinforced concrete frames by carbon fiber reinforced polymers under blast loading," *Cur Trends Civil & Structures Engineering*, vol. 2, no. 5, 2019.

[11] S. N. Malarvizhi, K. Ilamparuthi, and S. Bhuvaneshwari, "Behavior of geogrid encased stone column and stone column stabilized soft clay bed," in *Proceedings of the 6th International Conference on Physical Modelling in Geotechnics*, Hong Kong, China, August 2006.

[12] J. Hughes and N. Withers, "Reinforcing of soft cohesive soils with stone columns," *Ground Engineering*, vol. 7, no. 3, pp. 42–49, 1974.

[13] S. M. Seyed Kolbadi, N. Hassani, S. M. Seyed-Kolbadi, and M. Mirtaheri, "Analyzing parametric sensitivity on the cyclic behavior of steel shear walls," *Shock and Vibration*, vol. 2021, Article ID 3976793, 10 pages, 2021.

[14] D. McKelvey, V. Sivakumar, A. Bell, and J. Graham, "Modelling vibrated stone columns in soft clay," *Proc. Institution of Civil Engineers - Geotechnical Engineering*, vol. 157, no. 3, pp. 137–149, 2004.

[15] W. Hu, D. M. Wood, and W. Stewart, "Ground improvement using stone column foundations: result of model tests," in *Proceedings of the Int. Conf. on Ground Improvement Techniques*, pp. 247–256, CI-Premier, Singapore, 1997.

[16] S. Murugesan and K. Rajagopal, "Geosynthetic-encased stone columns: numerical evaluation," *Geotextiles and Geomembranes*, vol. 24, no. 6, pp. 349–358, 2006.

[17] W. Hu, *Physical modeling of group behavior of stone column foundations*, Ph.D. dissertation, Univ. of Glasgow, Glasgow, U.K, 1995.

[18] B. Mccabe, J. Mcneill, and J. Black, "Ground improvement using the vibro-stone column technique," in *Proceedings of the Transactions of the Institution of Engineers of Ireland*, Galway, January 2007.

[19] M. A. Hassan, M. A. M. Ismail, and H. H. Shaalan, "Numerical modeling for the effect of soil type on stability of embankment," *Civil Engineering Journal*, vol. 7, pp. 41–57, 2022.

[20] A. Zahmatkesh and J. Ch. Choobbasti, "Settlement evaluation of soft clay reinforced with stone columns using the equivalent secant modulus," *Arabian Journal of Geosciences*, vol. 5, no. 1, pp. 103–109, 2012.

[21] B. Mc Cabe, J. McNeill, and J. A. Black, "Ground improvement using the vibro stone column technique," in *Proceedings of the Institution of Engineers of Ireland*, Galway, January 2007.

[22] W. Mingming, C. Jianyun, W. Liang, and S. Bingyue, "Discussion of "hydrodynamic pressure on gravity dams with different heights and the westergaard correction formula"," *International Journal of Geomechanics*, vol. 22, no. 8, 2022.

[23] N. E. I. Boumekik, M. Labed, M. Mellas, and A. Mabrouki, "Optimization of the ultimate bearing capacity of reinforced soft soils through the concept of the critical length of stone columns," *Civil Engineering Journal*, vol. 7, no. 9, 2021.

[24] J. Lu, Z. Yang, K. Adlier, and A. Elgamal, "Numerical analysis ofstone column reinforced silty soil," in *Proceedings of the 15th Southeast Asian geotechnicalconference*, Bangkok, Thailand, November, 2004.